AIP Applied Physics Letters

On the origin of the redshift in the emission wavelength of InGaN/GaN blue light emitting diodes grown with a higher temperature interlayer

Z. G. Ju, S. T. Tan, Z.-H. Zhang, Y. Ji, Z. Kyaw et al.

Citation: Appl. Phys. Lett. **100**, 123503 (2012); doi: 10.1063/1.3694054
View online: http://dx.doi.org/10.1063/1.3694054
View Table of Contents: http://apl.aip.org/resource/1/APPLAB/v100/i12
Published by the American Institute of Physics.

On the origin of the redshift in the emission wavelength of InGaN/GaN blue light emitting diodes grown with a higher temperature interlayer

Z. G. Ju,[1] S. T. Tan,[1] Z.-H. Zhang,[1] Y. Ji,[1] Z. Kyaw,[1] Y. Dikme,[2] X. W. Sun,[1,3,a)] and H. V. Demir[1,4,5,b)]

[1]*LUMINOUS! Center of Excellence for Semiconductor Lighting and Displays, School of Electrical and Electronic Engineering, Nanyang Technological University, 50 Nanyang Avenue, Singapore 639798*
[2]*AIXaTech GmbH, Preusweg 109, 52074 Aachen, Germany*
[3]*Department of Applied Physics, College of Science and Tianjin Key Laboratory of Low-Dimensional Functional Material Physics and Fabrication Technology, Tianjin University, Tianjin 300072, China*
[4]*School of Physical and Mathematical Sciences, Nanyang Technological University, 50 Nanyang Avenue, Singapore 639798*
[5]*Departement of Electrical and Electronics Engineering, Department of Physics, and UNAM_Institute of Materials Science and Nanotechnology, Bilkent University, TR 06800 Ankara, Turkey*

(Received 19 January 2012; accepted 23 February 2012; published online 20 March 2012)

A redshift of the peak emission wavelength was observed in the blue light emitting diodes of InGaN/GaN grown with a higher temperature interlayer that was sandwiched between the low-temperature buffer layer and high-temperature unintentionally doped GaN layer. The effect of interlayer growth temperature on the emission wavelength was probed and studied by optical, structural, and electrical properties. Numerical studies on the effect of indium composition and quantum confinement Stark effect were also carried out to verify the experimental data. The results suggest that the redshift of the peak emission wavelength is originated from the enhanced indium incorporation, which results from the reduced strain during the growth of quantum wells. © *2012 American Institute of Physics*. [http://dx.doi.org/10.1063/1.3694054]

The peak emission wavelength of InGaN/GaN blue light-emitting diodes (LEDs) is one of the most important parameters for white LED applications.[1] For example, to effectively excite cerium (III)-doped YAG phosphors (yellow phosphors), it is required to design an InGaN/GaN blue LED that emits efficiently at 450–470 nm,[2] which corresponds to an indium composition of 15%–20%.[3] Typically, there are two ways to increase the indium incorporation during the quantum well (QW) growth. One is to lower the quantum well growth temperature to increase the indium/gallium ratio as indium has a lower vapor pressure than gallium. Another way is to suppress the composition pulling effect by prolonging the growth time and, thus, increasing the quantum well thickness.[4] However, the enhancement of indium composition through the above mentioned methods comes at a high cost of degradation of layer quality and hence, the device performance. Therefore, it is still challenging to grow high-quality quantum wells with a controllable indium incorporation.

On a separate issue, it is generally difficult to differentiate the effect of enhanced indium composition and the quantum confined Stark effect (QCSE) on the emission wavelength, both of which lead to redshift. QCSE arises from the polarization charges that are induced by the lattice mismatch of InGaN well and GaN barrier. The induced internal electric field shifts electrons and holes to the opposite sides of the well (i.e., separates the wave function of electrons and holes), in turn resulting in reduced recombination efficiency. Moreover, with a reduced overlap integral due to the strong polarization field, the effective bandgap of the QWs will shrink due to the tilted band edge. When the indium composition in an InGaN/GaN LED is increased, the QCSE increases as well. QCSE, together with the deteriorating crystal quality due to high indium composition, causes the efficiency degradation towards green emission, which is known as the "green gap" issue.[5] Hence, there is a need to study and understand the effect of the enhanced indium composition and QCSE on the LED performance.[6]

In this work, the redshift of emission wavelength was investigated in the InGaN/GaN blue LEDs grown under the same QW growth conditions but with a higher growth temperature of interlayer. The effects of the enhanced indium composition and QCSE on the performance of these LEDs were studied both experimentally and theoretically.

InGaN/GaN LEDs studied in this work were grown by an Aixtron Close Couple Showerhead metal-organic chemical-vapor deposition (MOCVD) system. Two-inch sapphire substrates with periodic cone patterns (with a diameter of 2.4 μm, a height of 1.5 μm, and a pitch of 3 μm) were used. The growth started with a 30 nm thick low-temperature u-GaN buffer grown at 560 °C, followed by a u-GaN interlayer ($\sim$150 nm thick) grown at different temperatures for different samples. Subsequently, a high-temperature u-GaN was grown at 1050 °C with a thickness of 5 μm and followed by a 2 μm Si-doped n-GaN at 1060 °C. Five pairs of multiple quantum wells (MQWs) with an undoped barrier were grown at 727 °C (samples LED I and LED II) and 737 °C (samples LED III and LED IV), with growth durations of 100 s and 110 s, respectively. The structures were finally covered with a 200 nm thick p-GaN grown at 950 °C and annealed at 685 °C. The key growth parameters are summarized in Table I, together with the full width at half maximum (FWHM) of the (002) and (102) x-ray diffraction (XRD) peaks. XRD was measured using Philips X'Pert XRD in a

[a)]Electronic mail: EXWSUN@ntu.edu.sg.
[b)]Electronic mail: HVDEMIR@ntu.edu.sg.

TABLE I. Growth parameters and FWHM values of XRD for LEDs I, II, III, and IV.

LED	Interlayer temperature (°C)	Quantum well temperature (°C)	Quantum well time (s)	FWHM (002) (arc sec)	FWHM (102) (arc sec)
I	930	727	100	207	291
II	950	727	100	186	230
III	970	737	110	188	192
IV	990	737	110	185	203

single axis scan mode. It can be seen from Table I that the crystal quality of the samples improves as the interlayer growth temperature was increased from 930 to 990 °C. FWHM values of (002) and (102) of the LED III and LED IV are both close to 200 arc sec, suggesting that the higher growth temperature of the interlayer could effectively reduce the dislocation density, especially the edge threading dislocation density.[7]

Photoluminescence (PL) spectra mapping were performed using a PL mapper (Nanometric RPM2000) equipped with a 15 mW He-Cd laser (325 nm) as the excitation source. Electroluminescence (EL) was tested on the epi-wafers using the 9 points Quick tester (M2442S-9A Quatek Group).

Figs. 1(a)–1(d) show the PL and EL spectra of LEDs I to IV, together with the PL mapping and 9-point EL data shown in the inset. The EL characteristics of the LEDs were performed at 9 points across the wafer with indium as both the p-type and n-type contacts. It can be seen from Fig. 1 that the LED II and LED IV, which have the same MQW growth condition but a higher interlayer growth temperature than LED I and LED III, respectively, show a redshift in their emission wavelengths for both PL and EL. With the same MQW growth condition, this redshift could potentially be due to (1) a higher indium composition in QWs or (2) a stronger polarization-induced QCSE.

Numerical simulations were carried out using Advanced Physical Models of Semiconductor Devices (APSYS) to verify the origin of the emission wavelength redshift. The simulator solves Schrödinger–Poisson equations self-consistently. The simulation has also taken Coulomb interaction into consideration with a typical dielectric constant of III-nitrides.[8] Since QCSE is determined by the internal electric field induced by both spontaneous polarization and piezoelectric polarization charge density (σ_{sp+pz}) in InGaN/GaN MQW active region, the macroscopic electrostatic field E can be expressed as follows:

$$E = -\frac{q}{\varepsilon_r \varepsilon_0}\sigma_{sp+pz}, \tag{1}$$

where σ_{sp+pz} is the total polarization charge density due to the dipoles along c-orientation, q is the elementary charge, ε_0 is the absolute dielectric constant, $\varepsilon_r = 1 + x$ is the relative dielectric constant, and x is the susceptibility for GaN.[9] Here, we simulate the LED structures to imitate the MOCVD-grown LED III and LED IV. A reference structure, LED S1 with an indium composition of 15% ($In_{0.15}Ga_{0.85}N$) and a typical polarization charge density of $4.0 \times 10^{12}\,cm^{-2}$ is used as a benchmark for LED III since they have nearly the same wavelength emission at a low current level. To account for the QCSE on the shift of the peak emission wavelength, LED S2 ($In_{0.15}Ga_{0.85}$ N) has a higher polarization charge density ($6.7 \times 10^{12}\,cm^{-2}$) but the same indium composition as compared to LED S1. On the other hand, LED S3 ($In_{0.16}Ga_{0.84}N$ with a polarization charge density of

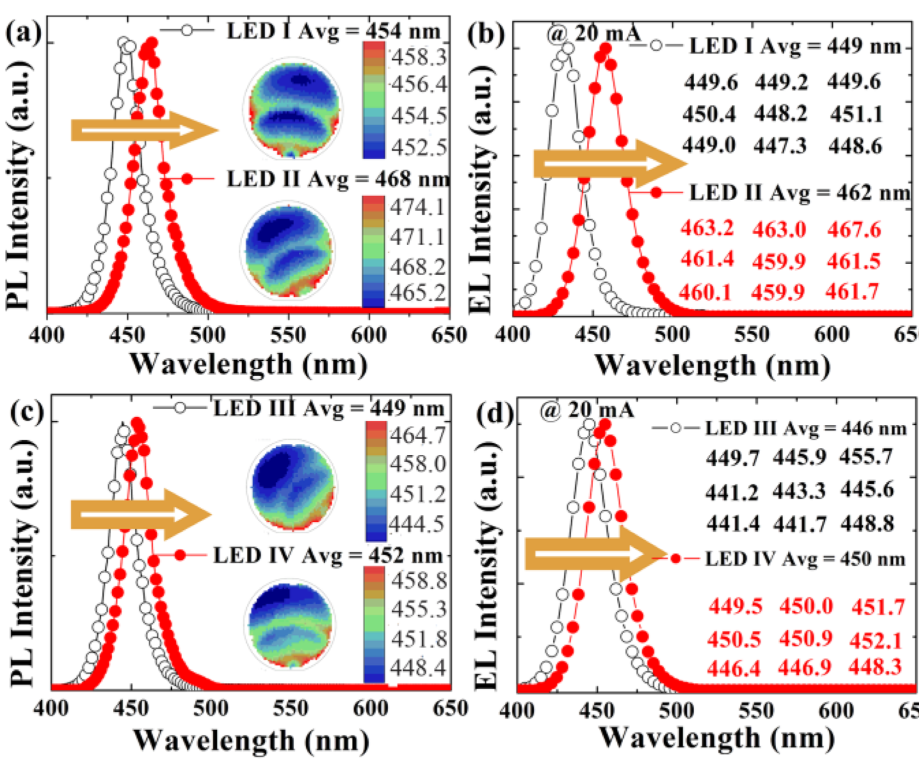

FIG. 1. (Color online) PL and EL spectra and mappings of the LEDs I, II, III, and IV.

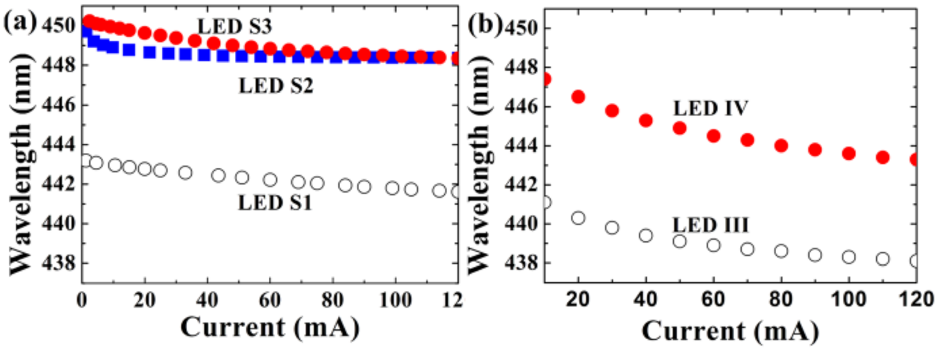

FIG. 2. (Color online) Peak emission wavelength versus injection current characteristics of (a) the simulated LEDs S1, S2, and S3 and (b) the experimentally characterized LEDs III and IV.

$4.0 \times 10^{12}\,\mathrm{cm}^{-2}$) was designed to account for the effect of the increased indium composition on the emission wavelength. The parameters assumed for LEDs S2 and S3 are based on the same emission wavelength at a low current injection level as the LED IV. Figs. 2(a) and 2(b) show the peak emission wavelength versus the injection current of the simulated LED structures (S1, S2, and S3), and the experimentally characterized LED structures (LED III and LED IV), respectively. As shown in Fig. 2(a), the rate of the wavelength change with increasing injection current for LED S2 and LED S3 is different especially in the low injection current regime. For LED S3, with a 1% higher indium composition as compared to LED S1, the emission wavelength blueshifts steadily with increasing injection current. On the other hand, LED S2, with a higher polarization charge density and, hence, a stronger QCSE as compared to LED S1, has a more drastic blueshift in the emission wavelength with increasing injection current at low current regime. Judging from the rate of the wavelength shift with increasing injection current, we can see that the LED IV (versus LED III) exhibits the same trend with LED S3 (versus LED S1), as shown in Figs. 2(a) and 2(b). Correspondingly, LED IV would have a higher indium composition in QWs as compared to LED III, even though both LEDs were grown under the same QW growth conditions. The observation for different shift rates of the emission wavelength with increasing injection current in LED S2 and LED S3 could be explained with the aid of screening effect to QCSE by free carriers or the band filling effect. It is noteworthy that the current density is low ($<1.0 \times 10^4$ mA/cm^2) in the electroluminescence measurement. Thus, the band filling effect is negligible and will not be considered in this case.[10] When the injection current increases, more free electrons and holes are generated, and this leads to a free-carrier-induced electric field to compensate with the piezoelectric field. Hence QCSE becomes smaller, the transition energy will become larger, and this causes a blue-shift of the emission peak wavelength.[11] Since stronger QCSE shows an obvious screening effect at low current level, LED S2 has a faster blue-shift trend in the emission wavelength at low current injection levels and then blue-shift slow until saturated even if injection current is further increased. However, for LED S3 with a weaker QCSE, the small screening effect will result in a longer process of continuous blue-shift with increasing current until the screening effect is saturated.

Fig. 3 shows the current-voltage and the current-power characteristics of LED III and LED IV. It is seen that LED IV has a lower turn-on voltage than LED III. This also suggests that LED IV has a lower built-in potential according to the diode current-voltage characteristics,

$$I = I_s(e^{q(V-V_{bi})/kT} - 1), \tag{2}$$

where I is the current, V is the applied voltage, V_{bi} is the built-in potential, I_s is the saturation current, q is the elementary charge, k is the Boltzmann constant, and T is the absolute temperature.[12] On the other hand, the built-in potential is proportional to the piezoelectric field and could be expressed as follows:

$$V_{bi} = E_i(d_u + d_d) + E_{pz} \cdot NL_w, \tag{3}$$

where E_{pz} is the piezoelectric field and E_i is the internal field in undoped and depletion regions.[13] The thickness of undoped region and depletion region, the number and the width of the QWs are represented by d_u, d_d, N, and L_w, respectively. By correlating Eqs. (2) and (3), it is possible to see that the turn-on voltage is proportional to the piezoelectric field and, hence, proportional to the QCSE. As a result, the lower turn-on voltage of LED IV, as compared to LED III, indicates that LED IV has a weaker or similar QCSE compared to LED III. In addition, it can also be observed from Fig. 3 that LED IV holds a higher output power than LED III, which also supports the argument that the QCSE in LED IV is weaker than that in LED III as QCSE will facilitate electron overflow, leading to reduction in optical power.[14]

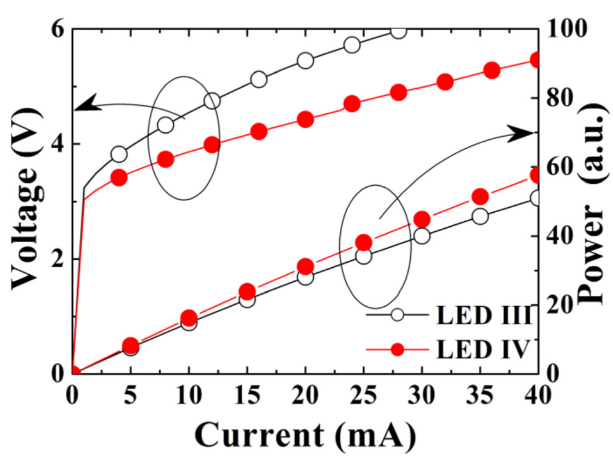

FIG. 3. (Color online) Current-voltage and current-power measurement of LEDs III and IV.

Judging from both the experimental and numerical results, the redshift of the peak emission wavelength in both LED II and LED IV, as compared to LED I and LED III, should step from the enhanced indium composition in QWs. The insertion of an interlayer sandwiched between the buffer layer and high-temperature u-GaN could generate tensile strain in the subsequent u-GaN layer. With the increasing growth temperature of the interlayer, it can further reduce the composition pulling effect.[4] This implies that the insertion of a high-temperature grown interlayer could generate more tensile strain,[15] which in turn compensates for the compressive strain induced by the incorporation of indium in the QWs.

In summary, the performance of InGaN/GaN LEDs was probed with optical, structural, and electrical characterization. The enhanced indium incorporation during the growth of quantum wells is found responsible for the redshift of the peak emission wavelength. The tensile strain generated by inserting a higher temperature interlayer helps to compensate for the compressive strain originating from InGaN/GaN, which in turn favors the incorporation of indium during the quantum well growth without increasing the QCSE and sacrificing the layer quality.

This work is supported by Singapore National Research Foundation, under Grant Nos. NRF-RF-2009-09 and NRF-CRP-6-2010-2, Singapore Agency for Science, Technology and Research (A*STAR) Science and Engineering Research Council Public Sector Fund Grant No. 0921010057, National Natural Science Foundation of China (NSFC) (project No. 61006037), and the Key Program of Tianjin Natural Research Foundation under Grant No. 11JCZDJC21900.

[1] F. A. Ponce and D. P. Bour, Nature **386**(6623), 351 (1997).
[2] X. Li, L. Guan, J. Y. An, L. T. Jin, Z. P. Yang, Y. M. Yang, P. L. Li, and G. S. Fu, Chin. Phys. Lett. **28**(2), 027805 (2011).
[3] K. Ya Ya and A. V. Zinovchuk, Semicond. Sci. Technol. **26**(9), 095007 (2011); Z.-Y. Li, W.-Y. Uen, M.-H. Lo, C.-H. Chiu, P.-C. Lin, C.-T. Hung, T.-C. Lu, H.-C. Kuo, S.-C. Wang, and Y.-C. Huang, J. Electrochem. Soc. **156**(2), H129 (2009).
[4] S. Pereira, M. R. Correia, E. Pereira, K. P. O'Donnell, C. Trager-Cowan, F. Sweeney, and E. Alves, Phys. Rev. B **64**(20), 205311 (2001).
[5] T. Langer, A. Kruse, F. Alexej Ketzer, A. Schwiegel, L. Hoffmann, H. Jönen, H. Bremers, U. Rossow, and A. Hangleiter, Phys. Status Solidi C **8**(7–8), 2170 (2011).
[6] J. H. Ryou, W. Lee, J. Limb, D. Yoo, J. P. Liu, R. D. Dupuis, Z. H. Wu, A. M. Fischer, and F. A. Ponce, Appl. Phys. Lett. **92**(10), 101113 (2008).
[7] C. Mo, W. Fang, Y. Pu, H. Liu, and F. Jiang, J. Cryst. Growth **285**(3), 312 (2005).
[8] L. Zhang, K. Ding, N. X. Liu, T. B. Wei, X. L. Ji, P. Ma, J. C. Yan, J. X. Wang, Y. P. Zeng, and J. M. Li, Appl. Phys. Lett. **98**(10), 101110 (2011).
[9] J. H. Ryou, P. D. Yoder, J. P. Liu, Z. Lochner, H. Kim, S. Choi, H. J. Kim, and R. D. Dupuis, IEEE J. Sel. Top. Quantum Electron. **15**(4), 1080 (2009).
[10] T. Kuroda and A. Tackeuchi, J. Appl. Phys. **92**(6), 3071 (2002).
[11] X. Wang, H. Qiang Jia, Y. Jiang, Z. Ma, Y. Chen, P. Xu, H. Li, T. He, L. Dai, and H. Chen, Proc. SPIE **7852**, 78520E (2010).
[12] E. F. Schubert, *Light Emitting Diodes*, 2nd edition (Cambridge University Press, Troy, New York, 2006).
[13] T. Takeuchi, C. Wetzel, S. Yamaguchi, H. Sakai, H. Amano, I. Akasaki, Y. Kaneko, S. Nakagawa, Y. Yamaoka, and N. Yamada, Appl. Phys. Lett. **73**(12), 1691 (1998).
[14] M. H. Kim, M. F. Schubert, Q. Dai, J. K. Kim, E. F. Schubert, J. Piprek, and Y. Park, Appl. Phys. Lett. **91**(18), 183507 (2007).
[15] H. Amano, M. Iwaya, T. Kashima, M. Katsuragawa, I. Akasaki, J. Han, S. Hearne, J. Floro, E. Chason, and J. Figiel, Jpn. J. Appl. Phys. **37**, L1540 (1998).